

Accepted Manuscript

The inhibitory role of curcumin derivatives on AMPA receptor subunits and their effect on the gating biophysical properties

Mohammad Qneibi, Othman Hamed, Oswa Fares, Nidal Jaradat, Abdel-Razzak Natsheh, Qais AbuHasan, Nour Emwas, Rana Al-Kerm, Rola Al-Kerm



PII: S0928-0987(19)30214-3
DOI: <https://doi.org/10.1016/j.ejps.2019.06.005>
Reference: PHASCI 4951

To appear in: *European Journal of Pharmaceutical Sciences*

Received date: 5 April 2019
Revised date: 17 May 2019
Accepted date: 3 June 2019

Please cite this article as: M. Qneibi, O. Hamed, O. Fares, et al., The inhibitory role of curcumin derivatives on AMPA receptor subunits and their effect on the gating biophysical properties, *European Journal of Pharmaceutical Sciences*, <https://doi.org/10.1016/j.ejps.2019.06.005>

This is a PDF file of an unedited manuscript that has been accepted for publication. As a service to our customers we are providing this early version of the manuscript. The manuscript will undergo copyediting, typesetting, and review of the resulting proof before it is published in its final form. Please note that during the production process errors may be discovered which could affect the content, and all legal disclaimers that apply to the journal pertain.

**The Inhibitory Role of Curcumin Derivatives on AMPA Receptor subunits and Their
Effect on the Gating Biophysical Properties.**

**Mohammad Qneibi^{a,*}, Othman Hamed^b, Oswa Fares^b, Nidal Jaradat^c, Abdel- Razzak
Natsheh^d, Qais AbuHasan^a, Nour Emwas^a, Rana Al-Kerm^b, Rola Al-Kerm^b**

^a Department of Biomedical Sciences, Faculty of Medicine and Health Sciences, An-Najah National University, Nablus, Palestine.

^b Department of Chemistry, Faculty of Science, An-Najah National University, Nablus, Palestine.

^c Department of Pharmacy, Faculty of Medicine and Health Sciences, An-Najah National University, Nablus, Palestine.

^d Department of Computer Information Systems, Faculty of Engineering and Information Technology, An-Najah National University, Nablus, Palestine.

*Corresponding author. Tel. +00-972-545 975 16; fax. +00-970-9 2345 982; E-mail address: mqneibi@najah.edu; Postal address: P.O.Box 7 Nablus-Palestine.

ABSTRACT

Curcumin is a natural polyphenol that has a broad spectrum of therapeutic characters, including neuroprotective actions against various neurological diseases. However, the molecular mechanism behind its neuroprotective properties remains obscure. The current study investigated the neuroprotective properties of 7 different curcumin derivatives on the gating biophysical properties of AMPA receptors, specifically on the calcium-permeable homomeric GluA1 and calcium impermeable heteromeric GluA1/A2 subunits. Due to the association between excessive activation of AMPARs and neurotoxicity linked to numerous pathologies, we aim to target and manipulate the kinetics of AMPARs through these derivatives. The current study used patch-clamp electrophysiology to measure the whole-cell currents in the presence and absence of the curcumin derivatives onto HEK293 cells expressing AMPA subunits. Our results showed that some of the curcumin derivatives showed an inhibitory effect and altered the gating biophysical properties, namely, deactivation and desensitization. In the presence of those derivatives, the peak current measured was significantly reduced, and the desensitization and deactivation rates decreased as well, achieving slower kinetics of the receptor and depressing its activity. These results suggest that the two most promising derivatives have inhibitory actions and act as allosteric modulators. Many neurological diseases like Epilepsy, ALS, and strokes are associated with overactivation of AMPA receptors. We can potentially synthesize a more potent neuroprotective drug to treat those neurological diseases, by understanding the most stable chemical interaction between the derivative and the receptor underlying the reported neuronal depressive properties.

Keywords: Neuroprotective; Curcumin Derivatives; AMPA Receptors; Activation; Desensitization; Deactivation.

1. Introduction

Curcumin is a natural polyphenol that has various effects on the body including anti-inflammatory, antioxidant, anti-cancer, and cardio-protective properties (Aggarwal et al., 2004; Hatcher et al., 2008; Maheshwari et al., 2006; Shishodia et al., 2005; Singh et al., 1998). Moreover, it has various effects on the central nervous including neuroprotective effects such as anti-protein-aggregation also has antioxidant, and anti-inflammatory activities (Bertoncello et al., 2018; Menon and Sudheer, 2007). Curcumin showed protective properties against glutamate excitotoxicity, which has been linked to various neurological diseases (Chen et al., 2015; Jayanarayanan et al., 2013; Matteucci et al., 2011) including epilepsy, Amyotrophic Lateral Sclerosis (ALS), Alzheimer's disease (AD), and strokes (Chang et al., 2012).

Glutamate, which is involved in neurotoxicity, mediates the majority of excitatory neurotransmission in the central nervous system (CNS) (Traynelis et al., 2010) and targets two families of receptors; the metabotropic (mGluRs) and ionotropic (iGluRs) Glutamate receptors (Simeone et al., 2004). The agonists AMPA, NMDA and Kainate target the three types of receptors composing iGluRs, which are α -amino-3-hydroxy-5-methyl-4-isoxazolepropionic acid receptor (AMPA), N-methyl-D-aspartate receptor (NMDAR) and Kainate receptor (Kew and Kemp, 2005). Although AMPA, kainite, and NMDA receptors share a similar amino acid sequence, they diverge in function (Herguedas et al., 2016). In addition, AMPAR mediates most of the fast-excitatory neurotransmission (Collingridge et al., 2009; Esteban, 2003) and plays a critical role in neuronal development and brain activities, such as learning and memory formation (Sanderson et al., 2008). Moreover, the activation of AMPARs are on a microsecond domain time scale, yet undergoes profound desensitization on the millisecond timescale. The kinetics of AMPARs, not only shape synaptic plasticity, determining long-term potentiation or

long-term depression, but also act as a neuroprotective mechanism against neurotoxicity (Kew and Kemp, 2005). These key features of AMPARs make them the focal point of interest in understanding various pathologies related to glutamate neurotoxicity as well as identifying inhibiting compounds that can modulate the kinetics of the receptor.

The composition of AMPARs at the synapse play a major role in its function depending on its pore-forming subunits (GluA1-4). Functional AMPA receptors are formed by the assembly of tetramers of one or more subunits or isoforms (Hollmann and Heinemann, 1994; Seeburg, 1993). The topology of any AMPA subunit can be divided into three domains; i. four hydrophobic domains, M1-M4 of which one is a re-entry loop, M2, while the rest are transmembrane domains, ii. a short intracellular cytoplasmic C-terminus and iii. An extracellular domain that consists of the N-terminal domain and the ligand binding domain. The segments of the extracellular domain between M3 and M4 are termed as S1 and S2 respectively have been shown to determine the specificity of agonist binding to AMPARs. (Herguedas et al., 2016; Schwenk et al., 2012; Sobolevsky et al., 2009; Sun et al., 2002).

Neurologic diseases have been treated using pharmacological drugs, however, despite modest efficacy, these drugs have several side effects including extrapyramidal symptoms, akathisia, tardive dyskinesia or the development of more serious conditions such as cardiac arrhythmias, severe neuroleptic syndrome and stroke (Brodaty et al., 2003; Ma et al., 2014). While AMPARs were studied, many ligands have been shown to possess selective inhibitory properties against them (Libbey et al., 2016; Nikam and Kornberg, 2001; Qneibi et al., 2012), therefore, efforts have been made to discover antagonists against AMPARs with better potency, specificity and longer duration of action.

Heterocyclic compounds are distinct regarding their biological activities, and they comprise a common structural unit of most marketed medicines. The capability of the drug in forming hydrogen bonds improves its solubility in hydrophilic solvents and the ability to interact with the bioactive sites. Given these facts and as a part of our ongoing studies on developing a new natural based drug, we decided to prepared curcumin derivatives with various heterocyclic moieties and evaluated their inhibitory role on AMPA Receptor. The type and size of a heterocyclic ring, in addition to the ring substituents, impact the biological activity of the compound (Broughton and Watson, 2004) strongly, three different types of heterocyclic moieties pyrazole, isoxazole, and diazepine was chosen for this purpose in addition to a Schiff base. These curcumin derivatives are accessible to synthesis and in a quantitative yield. Besides, benzodiazepines derivatives have been shown to exhibit desirable anticonvulsant and neuroprotective properties in cellular and animal models (1). Several pyrazole derivatives showed an excellent binding affinity for AMPA receptor (2). Also, compounds with isoxazole moiety showed high potency and selectivity toward AMPA antagonists (3). Regarding the Schiff base, the carbonyl groups in curcumin compounds are weak H-bonding acceptor, and one way of enhancing its potency and binding affinity toward AMPAR is by adding functionality that acts as an H-bonding donor and acceptor. The current study aims to investigate the effect of curcumin derivatives on the calcium impermeable homomeric GluA1 and calcium permeable heteromeric GluA1/A2 AMPA subunits in addition aims to assess the changes in the whole cell currents and AMPARs biophysical properties.

2. Results and discussion

2.1. Effect of curcumin derivatives on the peak current of AMPAR subunits

The effect of curcumin derivatives on the whole-cell current amplitude (A) was measured in the absence and presence of curcumin derivatives (A_i). To ensure an efficient, low-noise whole-cell recordings, the amplitude of both GluA1 and GluA1/A2 receptors was measured using Integrated Patch Amplifiers (IPA). For both AMPA receptors' subunits, we chose 10 mM for the high glutamate concentrations. This concentration corresponds to $\sim 95\%$ of the open-channel form (Qneibi et al., 2012). The Agonist was applied on AMPAR by using Fast Exchange solution i.e. Piezo. Cell currents were measured in the presence and absence of curcumin derivatives at a concentration of 20 μM , no change in the inhibition nor the biophysical properties above this concentration was noted. Data were analyzed using Igor 7 software.

For GluA1 homomer, the peak current for glutamate in the absence of any curcumin derivative was 774 ± 69 pA. Curcumin derivative CR-MeNH significantly decreased the peak current to 151 ± 13 pA and CR-NO decreased it to 146 ± 11 pA. While CR-NN and CR-NNPh showed the similar effect as CR-NN decreased peak current to 188 ± 39 pA and CR-NNPh decreased it to 302 ± 37 pA. However, curcumin, CR-PhCl, CR-PhF and CR-PhBr did not show significant change. The peak currents for those derivatives were 528 ± 45 pA, 759 ± 38 pA, 766 ± 26 pA, and 751 ± 38 pA, respectively.

For GluA1/A2, the peak current for glutamate in the absence of any curcumin derivative was 310 ± 53 pA. Curcumin derivative CR-MeNH significantly decreased the peak current to 54 ± 8.0 pA and CR-NO decreased it to 55 ± 6.4 pA. While CR-NN and CR-NNPh showed the similar effect as CR-NN decreased peak current from to 75 ± 7.0 pA and CR-NNPh decreased it to 105 ± 13 pA. However, curcumin, CR-PhCl, CR-PhF and CR-PhBr did not show significant change. The peak currents for those derivatives were 220 ± 31 pA, 298 ± 27 pA, 304 ± 41 pA, and 298 ± 26 pA, respectively.

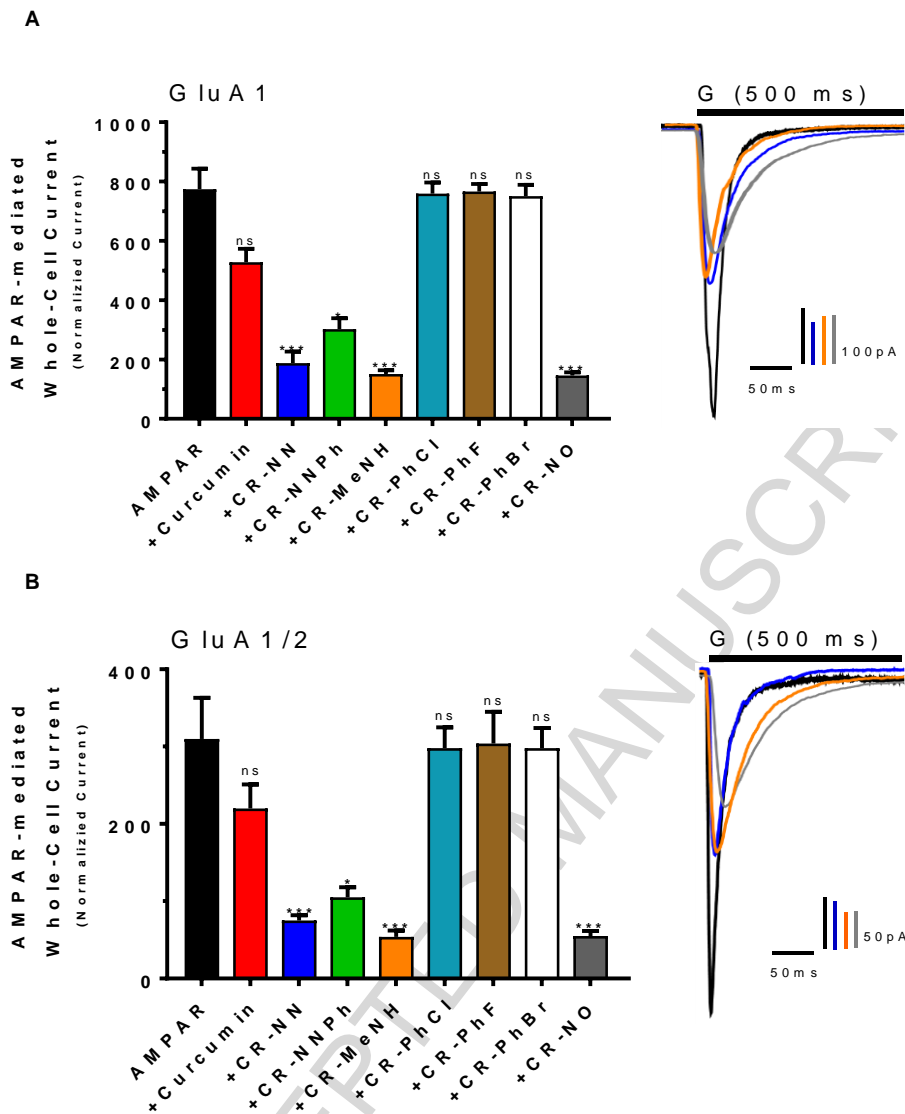


Fig. 2. Effect of curcumin and the derivatives on the amplitude of the whole-cell current with and without application of the derivatives.

The graphs (right) illustrate the peak current for the whole cell recordings of GluA1 (A) and GluA1/A2 (B) conducted at -60 mV, pH 7.4, and 22 °C, upon 500 ms application of 10 mM glutamate with and without curcumin derivatives. While on the left are above G current traces from HEK293 cells expressing homomeric GluA1 (A) and heteromeric GluA1/2 (B). For both A and B, the most potent derivatives to reduce peak current are CR-NN, CR-NNPh, CR-MeNH and CR-NO. Patches were repeated 5-7 times \pm SEM.

2.2. Curcumin derivatives alter AMPAR desensitization rate

The average desensitization time of GluA1 was 3.1 ± 0.1 ms denoting an average rate ($\tau=1/\text{ms}$) of 0.32 ms^{-1} . The derivative CR-MeNH and CR-NO significantly increased the average desensitization time from 3.1 ± 0.1 ms to 9.2 ± 0.7 ms decreasing the rate from 0.32 ms^{-1} to 0.11 ms^{-1} by ~ 2.9 folds, while CR-NO increased the desensitization time to 9.4 ± 0.9 ms, decreasing its rate 0.11 ms^{-1} by ~ 2.9 folds. Both CR-NN and CR-NNPh showed similar effects. CR-NN increased the average desensitization time from 3.1 ± 0.1 ms to 8.4 ± 0.7 ms decreasing the desensitization rate to 0.12 ms^{-1} by ~ 2.6 folds and CR-NNPh increased the desensitization time to 7.1 ± 0.5 ms decreasing its rate to 0.14 ms^{-1} by ~ 2.3 folds. However, curcumin, CR-PhCl, CR-PhF and CR-PhBr did not show significant change. The average desensitization time for those derivatives was 3.9 ± 0.9 ms, 2.9 ± 0.9 ms, 2.9 ± 0.8 ms and 3.2 ± 0.7 ms, respectively.

For GluA1/A2, the average desensitization time was 5.4 ± 0.6 ms with a rate of 0.19 ms^{-1} . Curcumin derivative CR-MeNH significantly increased the average desensitization time from 5.4 ± 0.6 ms to 13.2 ± 2.9 ms decreasing the rate from 0.19 ms^{-1} to 0.08 ms^{-1} by ~ 2.4 folds while CR-NO increased the average desensitization time to 14.4 ± 3.4 ms, decreasing the desensitization rate to 0.07 ms^{-1} by ~ 2.7 folds. Both CR-NN and CR-NNPh showed similar effects. CR-NN increased the average desensitization time from 5.4 ± 0.6 ms to 10.2 ± 1.4 ms decreasing the rate from 0.19 ms^{-1} to 0.1 ms^{-1} by ~ 1.9 folds and CR-NNPh increased the desensitization time to 8.7 ± 1.2 ms, decreasing the rate to 0.11 ms^{-1} by ~ 1.7 folds. However, curcumin, CR-PhCl, CR-PhF and CR-PhBr did not show significant change. The average desensitization time for those derivatives was 5.4 ± 0.6 ms, 5.2 ± 0.9 ms, 5.2 ± 0.4 ms and 5.6 ± 0.3 ms, respectively.

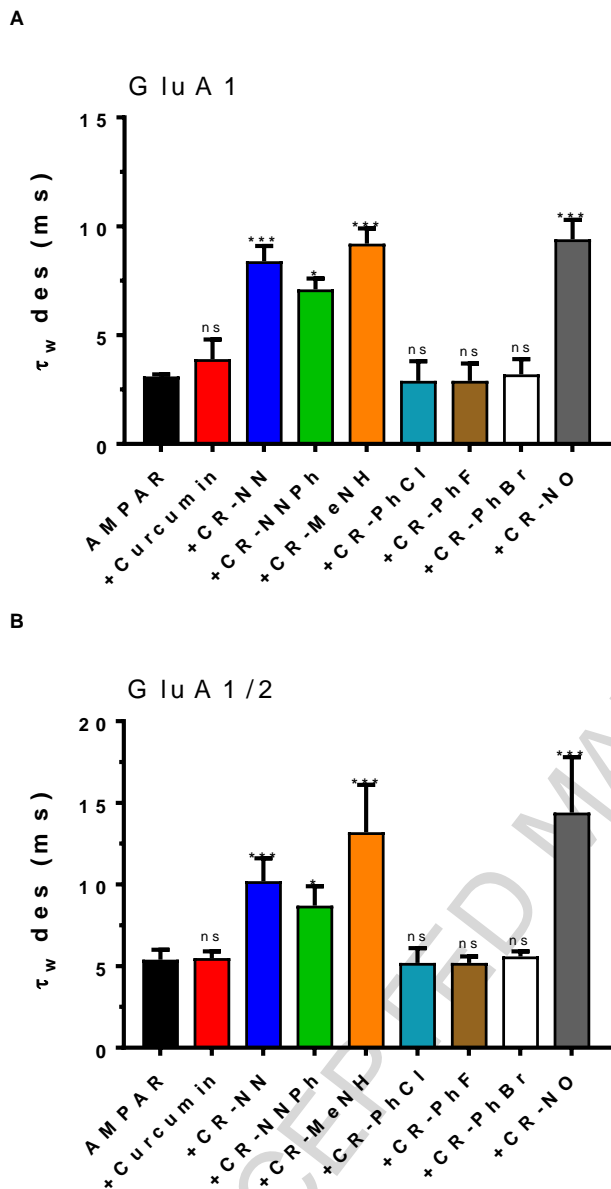


Fig. 3. Impact of curcumin and the derivatives on AMPAR desensitization. Graphs summarize weighted time constants for desensitization ($\tau_{w \text{ des}}$) for the whole cell recordings of GluA1 (A) and GluA1/A2 (B) conducted at -60 mV, pH 7.4, and 22 °C, upon 500 ms application of 10 mM glutamate with and without curcumin derivatives. For both A and B, the most potent derivatives to reduce the desensitization rate are CR-NN, CR-NNPh, CR-MeNH and CR-NO. Patches were repeated 5-7 times \pm SEM.

2.3. Curcumin derivatives modify AMPAR deactivation rate

The effects of curcumin on AMPAR's desensitization kinetics motivated the investigation of Curcumin derivatives on AMPAR deactivation (Fig. 4). The average deactivation time for GluA1 was 2.4 ± 0.1 ms which denotes a rate of 0.42 ms^{-1} . Curcumin derivative CR-MeNH significantly increased the average deactivation time from 2.4 ± 0.1 ms to 7.3 ± 0.6 ms, decreasing the deactivation rate from 0.42 ms^{-1} to 0.14 ms^{-1} by ~3 folds, while CR-NO increased it to 7.5 ± 0.7 ms, decreasing the rate to 0.13 ms^{-1} by ~3.2 folds. CR-NN and CR-NNPh showed the similar effect as CR-NN increased the average deactivation time from 2.4 ± 0.1 ms to 6.5 ± 0.4 ms decreasing the deactivation rate from 0.42 ms^{-1} to 0.15 ms^{-1} by ~2.8 folds and CR-NNPh increased the deactivation time to 5.1 ± 0.4 ms, decreasing the rate to 0.2 ms^{-1} by ~2 folds. However, curcumin, CR-PhCl, CR-PhF and CR-PhBr did not show significant change. The average deactivation time for those derivatives was 3.1 ± 0.3 ms, 2.5 ± 0.6 ms, 2.3 ± 1.0 ms and 2.6 ± 0.4 ms, respectively.

For GluA1/A2, the average deactivation time was 2.3 ± 0.1 ms with an average deactivation rate of 0.43 ms^{-1} . The derivative CR-MeNH significantly increased the average deactivation time from 2.3 ± 0.1 ms to 8.3 ± 0.8 ms decreasing the rate from 0.43 ms^{-1} to 0.12 ms^{-1} by ~3.6 folds and CR-NO increased the deactivation time to 8.8 ± 0.7 ms, decreasing the rate to 0.11 ms^{-1} by ~3.9 folds. While CR-NN and CR-NNPh showed similar effects as CR-NN increased the average deactivation time from 2.3 ± 0.1 ms to 7.8 ± 0.6 ms decreasing the rates from 0.43 to 0.13 by ~3.3 folds and CR-NNPh decreased the deactivation time to 6.6 ± 0.9 ms, decreasing its rate to 0.15 by ~2.9 folds. However, curcumin, CR-PhCl, CR-PhF and CR-PhBr did not show significant change. The average deactivation time for those derivatives was 2.8 ± 0.3 ms, 2.2 ± 0.5 ms, 2.1 ± 0.7 ms and 2.5 ± 0.5 ms, respectively.

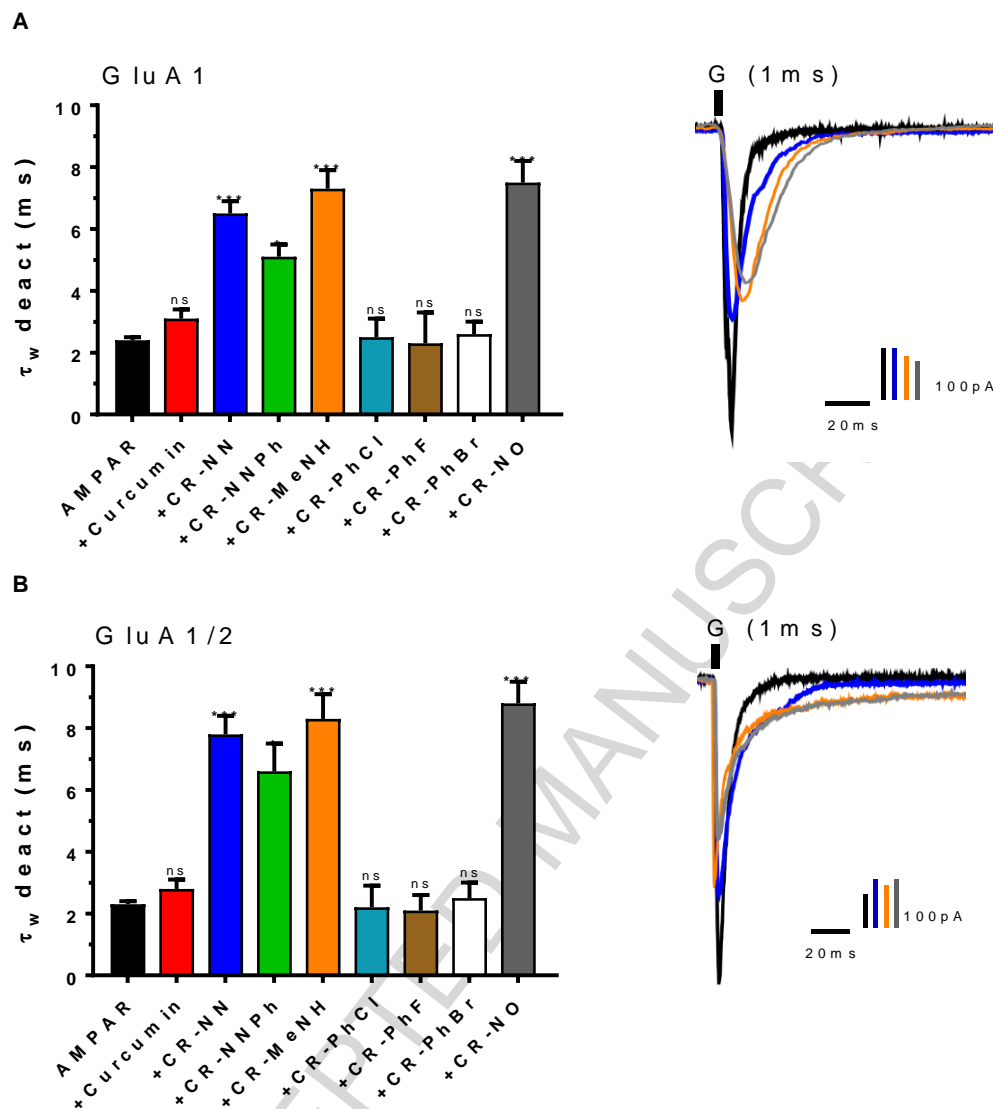


Fig. 4. Results of Curcumin and the derivatives effect on AMPAR deactivation. The Graphs on the right summarize weighted time constants for deactivation (τ_w deact) for the whole cell recordings of GluA1 (A) and GluA1/A2 (B) conducted at -60 mV, pH 7.4, and 22 °C, upon 500 ms application of 10 mM glutamate with and without curcumin derivatives. While on the left are above G current traces from HEK293 cells expressing homomeric GluA1 (A) and heteromeric GluA1/2 (B). For both A and B, the most potent derivatives to reduce deactivation rates are CR-NN, CR-NNPh, CR-MeNH and CR-NO. Patches were repeated 5-7 times \pm SEM.

The activation of AMPARs results in transforming a chemical signal into an electrical one, as it takes place after the binding of glutamate to the receptor leading to the opening of a transmembrane ion channel and allowing ion influx into the neuron. The work of Armstrong and Mayer in 2004 provided structural data at atomic resolution for S1 and S2 domain, which revealed their separation by the membrane regions M1 to M3. Moreover, it was demonstrated that in an intact receptor the functional folding of AMPARs created two globular domains, referred to as D1 and D2, extracellularly that play a major role in both activation and desensitization. Hence, accumulating evidence shows the rotational changes between the dimers upon agonist binding, which in return, influence the activation of the receptor. The structural mechanism of channel opening and activation upon agonist binding to S1 and S2 has been widely accepted to be associated with conformational changes in the extracellular domains. Yet, the mechanism controlling the transduction of these conformation changes to channel gating remain to be obscure. Although, it is believed to involve linker regions between TMD and LBD, namely the S1-M1, S2-M3, and S2-M4 linkers (Balannik et al., 2005; Twomey and Sobolevsky, 2018; Wang et al., 2014; Yelshanskaya et al., 2016).

Rearrangement of the extracellular dimer interface has also been identified in relation to the desensitization of the receptor. Unlike deactivation, which is the natural decay in current after a short simulation time following activation at which the ligand unbinds from the receptor, desensitization is a long simulation time decay in current following long activation with the ligand remaining to be bound to the receptor (Akhondzadeh and Abbasi, 2006; Vickers et al., 2001). As a consequence the flow of ion into the neuron through AMPARs is terminated via deactivation or desensitization. A structural mechanism of desensitization was provided by Yu Sun in 2002, which explained that the conformation stability of desensitization is higher than that

of the activation state. It was found that upon agonist binding, the opening of the channel was coupled with a separation of the linker regions, yet this required a stable dimer interface (Sun et al., 2002; Twomey and Sobolevsky, 2018). Correctly, the channel opens as the gate receives a conformational strain, which has been caused by domain closure, due to agonist binding. However, during desensitization, the dimer interface rearranges, therefore no observable conformational strains are being transmitted to the ion channel gate, as a result, the domain closure is decoupled from the channel gate. Both desensitization and deactivation are potential targets to manipulate the strength of AMPAR signal transmission, to treat various diseases that are associated with excessive activation and intense signalling transduction from AMPARs. The current study synthesizes different curcumin derivatives as shown in Fig. 1 and investigate their effects on the electrophysiology mediated by AMPA glutamate receptors. Their effects were investigated using biochemical and electrophysiologic approaches by characterizing the effect on AMPA receptors kinetics (i.e., peak current, desensitization, and deactivation), and detecting any modulatory activity.

For both GluA1 homomer and GluA1/A2 heteromer, CR-MeNH and CR-NO showed the most significant inhibitory effect by reducing the peak current by 5 folds. They also reduced both deactivation and desensitization rates remarkably by at least 3 and 2 folds, respectively, denoting the property to slow the kinetics of those receptors. Likewise, CR-NN and CR-NNPh had similar impact on both receptors by decreasing the peak current and increasing the duration of the state at which the receptor is desensitized or deactivated. However, Curcumin, CR-PhCl, CR-PhF and CR-PhBr did not show significant changes in the peak current, deactivation or desensitization. Our results regarding curcumin align with (Nelson et al., 2017) study that provides evidence to classify curcumin as PAINS (pan-assay interference compounds) and an IMPS (invalid

metabolic panaceas) candidate, as it had no effect on any of the tested biophysical properties nor show any inhibition on either receptors.

The effect of CR-NN, CR-NNPh, CR-MeNH and CR-NO on the peak current of the receptor reveal a decrease in activation, insinuating that the active sites of these compounds have an affinity to an inhibitory binding site on the receptor. An increase in glutamate concentration had no observable effect on derivative concentrations, meaning they act as noncompetitive inhibitors. In accordance with various research on non-competitive antagonist, such as, the derivatives of 2,3-benzodiazepine, PMP, and CP, the interaction occurs in the linker regions, specifically S1-M1 and S2-M4 linkers (Balannik et al., 2005) (Fig. S1).

As shown above, curcumin derivatives with five-membered ring heterocyclic moiety showed excellent inhibition activities. The results could be explained based on structure activity-relationship hypothesis.³¹ The size isoxazole and pyrazoles derivatives and the presence of the heteroatoms (O, N) at positions 1 and 2 give the molecules the ability to accommodate well into the binding pocket and interact with the receptor site as an H-bonding acceptor. Curcumin amino compound CR-MeNH showed the highest inhibition activity. The size of the molecule and the presence of the free amino groups give the molecule the ability to better fit in the binding pocket and the strong capability to physically bond as H-bond acceptor and donor with the receptor site. However, the benzodiazepines derivatives showed no activities. This could be attributed to the hindrance of the molecule, due to the presence of the phenyl group, which is bonded from two sites; 1 and 2. The hindrance is incapable of fitting into the binding site, thus affecting the contact with the active functionality surrounding the active sites in the binding pocket. The location of the heteroatoms at 1,4 positions, could affect the molecular contact between the receptor sites of the pockets and the ring heteroatoms. Besides, the phenyl group acts as an

electron withdrawing group, thus reducing the strength of H-bonding that might form between the amino groups of the benzodiazepine and pocket active sites. Based on the obtained results and the explanation we offered, we speculate that, compounds such as curcumin amine 2 (Fig. 1) could show the highest binding potency and thus provide the highest inhibition activities. Unfortunately, so far, we were not succeeding in preparing the curcumin amine compound.

The work of (Balannik et al., 2005) in mutagenesis research, an attempt to decode the structural mechanism involved in noncompetitive inhibition, reveals the function of the inhibitors as blocking the transmission of conformational changes in the LBD to D2, by acting as a wedge (Twomey and Sobolevsky, 2018; Yelshanskaya et al., 2016). Moreover, as the inhibitor binds entirely to the binding pocket of the receptor, conformational changes in the TMD is accompanied, specifically at pre-M1/M1, M3, and M4, which have been further separated (Yelshanskaya et al., 2016). Although various residues play a vital role in the binding pocket, their role is dependent on the chemical structure of the inhibitor. Since CR-MeNH and CR-NO had the most impact on both activation and desensitization, we assume the residues to be involved are central for both activation and desensitization. Hence, the binding of the derivative acts against the separation of linkers that are coupled with agonist binding for receptor opening, but also stabilizing the desensitized and deactivated state of the receptors.

The results of the current study were independent of subunit makeup of the receptor as they shared similar significant changes between the homomeric and heteromeric subunit. Previous studies indicated that the residues on the AMPA receptor at the location of antagonist binding seems to be shared throughout all of AMPA subunits; hence the binding affinity depends on the chemical structure of the inhibitor (Balannik et al., 2005; Yelshanskaya et al., 2016). Depressing the activity of those receptors has therapeutic effects on various disorders and CR-NN, CR-

NNPh, CR-MeNH and CR-NO show such property that could be promising for future drug synthesis. Moreover, the different results achieved using the curcumin derivatives shed light on the possible effects of changing the chemical compositions and achieving a better understanding of the receptors' binding sites affinity to such changes.

3. Conclusion

In conclusion, the current study demonstrated that the two-curcumin derivative CR-MeNH and CR-NO had the most potent effects on AMPAR kinetics in comparison to the other tested curcumin derivatives. The effects observed on AMPAR kinetics in our results revealed a decrease in desensitization and deactivation rate, as well as a decrease in activation, suggesting that the derivatives modify the AMPAR gating kinetics by the direct contact and association with AMPA receptors. Furthermore, these derivatives act as noncompetitive inhibitors making AMPA receptors less sensitive for its agonist glutamate. We propose three different mechanisms for the observed effects of CR-MeNH and CR-NO on AMPAR kinetics; first, the derivatives might affect AMPAR trafficking, reducing AMPAR density on the postsynaptic cleft. Second, they might alter the chemical structure of the pore-forming groups of the AMPAR ion channel, changing their electrochemical permeability to specific ions. Third, by acting as antagonistic modulators, they bind to allosteric sites that, in return, affect AMPAR conformation, stabilizing the desensitized and deactivation conformations and hindering activation. These results are promising in comparison to alternative pharmacological treatment, as the derivatives of a natural polyphenol will demonstrate lower side effects.

For future research, we aim to investigate the effects of these derivatives on calcium impermeable GluA2 containing AMPA subunits and design a better understanding of noncompetitive structural inhibition. This study specifically looks at curcumin derivatives

influencing the biophysical gating properties of both homomeric and heteromeric AMPA subunits, yet further research is needed to understand the specific interaction between the receptor and the derivative and the mechanism of impact to potentially synthesize a non-competitive inhibitory drug against AMPARs to treat the diseases that have been linked to excessive AMPA activity.

4. Experimental section

The curcumin derivatives chosen for this work and a future study (figure 1) are; 4,4'-((1E,1'E)-isoxazole-3,5-diylbis(ethene-2,1-diyl))bis(2-methoxyphenol), 4,4'-((1E,1'E)-(1H-pyrazole-3,5-diyl)bis(ethene-2,1-diyl))bis(2-methoxyphenol), 4,4'-((3Z,5E)-3-(methylamino)-5-(methylimino)hept-3-ene-1,7-diyl)bis(2-methoxyphenol), 4,4'-((1E,1'E)-(7-chloro-3H-benzo[b][1,4]diazepine-2,4-diyl)bis(ethene-2,1-diyl))bis(2-methoxyphenol), 4,4'-((1E,1'E)-(7-fluoro-3H-benzo[b][1,4]diazepine-2,4-diyl)bis(ethene-2,1-diyl))bis(2-methoxyphenol), 4,4'-((1E,1'E)-(7-bromo-3H-benzo[b][1,4]diazepine-2,4-diyl)bis(ethene-2,1-diyl))bis(2-methoxyphenol) and 1-phenyl-3,5-bis-2-(4-hydroxy-3-methoxystyryl)-1H-pyrazole, for the sake of simplicity, the derivatives were abbreviated as; (CR-NO), (CR-NN), (CR-MeNH), (CR-PhCl), (CR-PhF), (CR-PhBr), and (CR-NNPh), respectively. The curcumin derivatives with five membered heterocyclic rings were prepared according to a published procedure (Hamed et al., 2013).

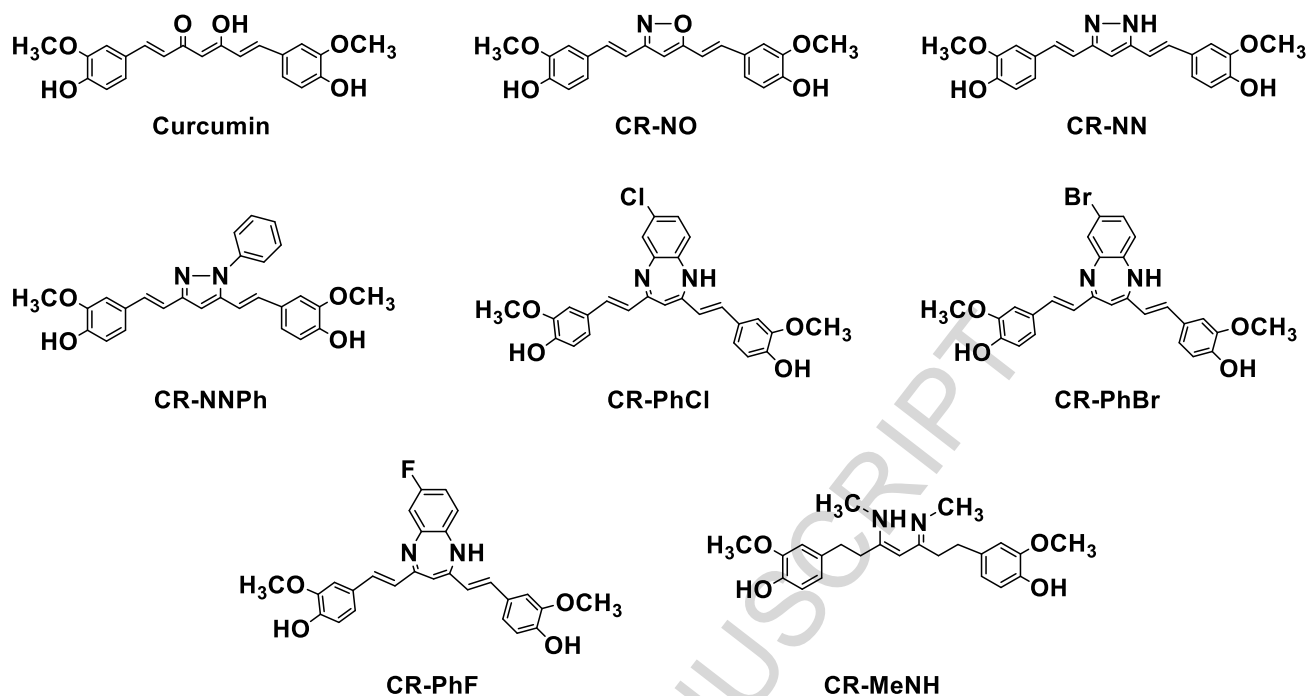


Fig. 1. The chemical structures of the prepared curcumin derivatives.

All chemicals used in this study were purchased from Aldrich Chemical Company and used as they were received. All prepared compounds were characterized by MS/MS, ^1H NMR, ^{13}C NMR, IR spectroscopy. Mass spectroscopic analysis was performed on solutions of compounds in a Nano scale concentration using a multi dilution procedure. The MS/MS was performed on LCQ Fleet ion trap mass spectrometer (Thermo Fisher Scientific, CA, USA) operated in a positive electrospray mode. The electrospray voltage was 5 kV. The capillary temperature was 290°C and the sheath gas flow was 30 units. An isolation width of 2 Da was used with a 20 msec activation time for MS experiments. All scan events were acquired with a 250 ms maximum ionization time. Nuclear Magnetic Resonance spectra were recorded on Varian Gemini 2000, 300 MHz instrument MHz instruments. Infrared spectra were recorded on a Shimadzu 820 PC FT-IR spectrometer. Solvent used in the NMR was DMSO- d_6 , ^1H NMR experiments were reported in δ units, parts per million (ppm) downfield from tetramethyl silane (TMS). All ^{13}C NMR spectra

were reported in ppm relative to DMSO-d₆ (39.52 ppm). TLC analysis was performed on silica gel plates pre-coated with Merck Kieselgel 60 F254 and visualization was done using UV lamp. Samples purifications were carried out by either crystallization or by flash chromatography with silica gel (100-200) mesh.

4.1. General experimental procedure for the preparation curcumin with 5-membered ring heterocyclic moiety

To a round bottom flask equipped with magnetic stirring bar and a condenser, curcumin (3.0 mmole, 1.1 g) was added followed with 20.0 mL acetic acid. The desired reagent of hydrazine (3.0 mmole) or hydroxyl amine was added to the solution of curcumin. The reaction mixture was refluxed for 6 h. The reaction mixture was concentrated *in-vacuo*, and re-dissolved in ethyl acetate (50 mL). The ethyl acetate layer was washed with saturated solution of NaHCO₃, saturated solution of NaCl and water. Then it was dried over Na₂SO₄ and concentrated *in-vacuo*. The produced solid was collected by suction filtration.

4.2. 1-phenyl-3,5-bis-2-(4-hydroxy-3-methoxystyryl)-1H-pyrazole (CR-NNPh)

Yield 71.6% (0.96 g), mp 127-129°C, IR: V_{\max} cm⁻¹ 3550 (-C-OH), 3345 (-C-NH), 3100, 1625 (-C=N), 1610, 1585 (C=C, Ph) and 1080 (C-O ether) of (-O-CH₃). ¹H-NMR (300 MHz, CDCl₃) δ ppm: 3.93 (s, 6H, OCH₃), 6.07 (s, 2H, OH), 6.82 (s, 1H, C4-H), 7.05 (d, 2H, J = 14.9 Hz, C2-H and, C6-H), 7.13 (d, 2H, J = 14.9 Hz, C1-H and C7-H), 7.15–7.33 (m, 8H, Ph-H), 7.45 (m, 2H, Ph-H), 7.72 (m, 1H, Ph-H). ¹³C NMR (300 MHz, CDCl₃) δ ppm: (300 MHz, CDCl₃): 56.1, 56.1, 101.2, 110.0, 111.0, 112.7, 116.1, 116.2, 117.5, 120.7, 125.2, 128.2, 128.3, 128.8, 129.0, 129.1, 129.1, 131.2, 133.3, 139.7, 142.8, 147.3, 147.8, 148.1, 148.3, 151.5, 161.2. Anal. Calcd for C₂₇H₂₄N₂O₄: C 73.62, H 5.49, N 6.36. Found: C 73.43, H 5.42, N 6.48.

4.3. 4,4'-((1E,1'E)-isoxazole-3,5-diylbis(ethene-2,1-diyl))bis(2-methoxyphenol) (CR-NO)

Yield 72.0 (0.8 g), mp 116-119°C, IR: V_{\max} cm^{-1} 3560 (-C-OH), 3035, 1640 (C=N), 1605 (C=C, 1586 (-C=C, Ph), 1330 (C-O of the five-member ring) cm^{-1} . $^1\text{H-NMR}$ (400 MHz, DMSO- d_6): $^1\text{H-NMR}$: δ 3.85 (s, 6H, 2OCH₃), 6.25 (s, 2H, OH), 6.71 (s, 1H, C4-H), 6.84-7.01 (m, 3H), 7.04-7.15 (m, 4H), 7.26 (m, 3H). $^{13}\text{C-NMR}$ (300 MHz, CDCl₃) δ ppm: 56.14, 56.18, 98.33, 110.56, 110.82, 113.12, 113.43, 115.98, 116.11, 116.24, 121.8, 122.16, 127.49, 127.83, 129.22, 135.27, 135.98, 148.22, 148.42, 162.70, 168.84. Anal. Calcd for C₂₁H₁₉NO₅: C 69.03, H 5.24, N 3.38. Found: C 68.89, H 5.21, N 3.41.

4.4. 4,4'-((1E,1'E)-(1H-pyrazole-3,5-diyl))bis(ethene-2,1-diyl))bis(2-methoxyphenol) (CR-NN)

Yield 72.0 (0.8 g), mp 116-119°C, IR: 3545 (-C-OH), 3035, 1640 (C=N), 1608, 1560 (-C=C, Ph), 1331 (C-O of the five-member ring) cm^{-1} . $^1\text{H-NMR}$ (400 MHz, DMSO- d_6): $^1\text{H-NMR}$: δ 3.83 (s, 6H, 2OCH₃), 6.25 (s, 2H, OH), 6.75 (s, 1H, C4-H), 6.81-7.07 (m, 3H), 7.07-7.16(m, 4H), 7.31 (m, 3H). $^{13}\text{C-NMR}$ (300 MHz, CDCl₃) δ ppm: 56.1, 56.1, 98.4, 110.7, 110.8, 113.1, 113.5, 115.98, 116.1, 116.2, 121.8, 122.2, 127.6, 127.8, 129.2, 135.3, 135.8, 148.2, 148.4, 162.7, 168.85. Anal. Calculated for C₂₁H₁₉NO₅: C 69.03, H 5.24, N 3.38. Found: C 68.89, H 5.21, N 3.41.

4.5. 4,4'-((3Z,5E)-3-(methylamino)-5-(methylimino)hept-3-ene-1,7-diyl))bis(2-methoxyphenol) (CR-MeNH)

Curcumin (1.0 g, 2.7 mmol) was dissolved in 50 mL of ethanol. The mixture was stirred until a clear solution was obtained. Methylamine solution 40% (0.465 g, 6 mmol) was added to the solution and the reaction mixture was refluxed for 2 h. The solvent was evaporated under vacuum, the residue was washed with 5% Na₂CO₃, water and dried. The residue was recrystallized from ethanol/water solution (1:2 by volume). Yield 64% (0.68 g), mp 171-175 °C.

IR: ν_{\max} cm^{-1} 3602 (-C-OH), 3050 (=C-H), 2943 (C-H), 1630 (C=N), 1610 (-C=C), 1580 (C=C, Ph), 1514, 1276, 1213, 1031. $^1\text{H-NMR}$ (400 MHz, DMSO- d_6): $^1\text{H-NMR}$ (Fig. 2.13): δ 2.86 (s, 6H, 2 NCH₃), 3.83 (s, 6H, 2OCH₃), 6.27 (s, 2H, OH), 6.69 (s, 1H, C4-H), 6.79-7.05 (m, 3H), 7.06-7.19 (m, 4H), 7.28 (m, 3H). $^{13}\text{C-NMR}$ (300 MHz, CDCl₃) δ ppm: 31.8, 39.6, 56.24, 56.17, 98.41, 110.67, 110.93, 113.23, 113.31, 116.02, 116.32, 116.25, 121.91, 122.17, 127.52, 127.93, 129.19, 135.15, 136.06, 148.31, 148.43, 162.75, 168.8.

4.6. DNA preparation

High-copy plasmid DNA (up to 20 μg) was prepared using QIAGEN Plasmid Mini Kit. A selective plate was streaked followed by the selection of a single colony. LB medium containing appropriate selective antibiotic was used for the starter culture inoculation. Incubation of the culture was for approximately 8 hours at 37°C, later diluted in 3 ml selective LB medium, then incubated at 37°C for 12-16 hours. The tube was centrifuged after which the formed pellet was resuspended to harvest the bacterial cells. 0.3 ml of buffer P2 was added to the tube; then it was inverted 4-6 times to homogenously mixing the contents. The tube was centrifuged and the supernatant containing the plasmid DNA was obtained.

A QIAGEN-tip 20 was equilibrated using 1 ml buffer QBT; the column was left to empty by gravity flow. The supernatant was added to the QIAGEN-tip 20, under gravity flow, it entered the resin. Then the QIAGEN-tip 20 was washed with buffer QC. The DNA was eluted with 0.8 ml buffer QF. For precipitation, isopropanol was added, mixed and centrifuged, then immediately and carefully, the supernatant was decanted. The resultant DNA pellet was washed with Ethanol, centrifuged again and the supernatant was decanted. Finally, the pellet was air-dried, and the DNA was re-dissolved in a suitable volume of buffer. To calculate DNA concentration both Bot spectrophotometry at 260 nm and quantitative analysis on an agarose gel

were used. The reliability of spectrophotometric DNA quantification was determined by A260 readings between the values of 0.1 and 1.0.

4.7. HEK293 Cell Culture and Transfection

Human Embryonic Kidney cells 293 (HEK293) were grown in Dulbecco Modified Eagle Medium (DMEM) (Sigma, USA) containing 10% FBS (fetal bovine serum), 0.1 mg/ml streptomycin, and 1 mM sodium pyruvate (Biological Industries; Beit-Haemek, Israel). HEK293 cells were incubated at 37° C and 5% CO₂ was supplemented to the medium (Li et al., 2003). It was subcultured twice a week until cells reached pass #20. The transfection reagent used was either jetPRIME (Polyplus: New York, NY) or Lipofectamine 2000 (Invitrogen; San Diego, CA) (Huang et al., 2005). Cells were kept for 24 hours after transfection then replated on coverslips coated with Laminin (1 mg/mL; Sigma, Germany) to use for electrophysiology recordings or stereomicroscope imaging.

4.8. HEK293 Cell Patch-Clamp Recordings

Using IPA (Integrated Patch Amplifier) (Sutter Instruments, Novato, CA) on the whole cell configuration of the patch-clamp technique, HEK293 Cells were recorded 36-48 hours after transfection, at a temperature of 22°C, the membrane potential of -60 mV. SutterPatch Software v. 1.1.1 (Sutter Instruments) to digitize membrane currents for a short period. Sampling frequency was set to 10 kHz, and the low-pass filter was set to 2 kHz. Borosilicate glass was used to fabricate the Patch electrodes with a resistance of 2-4 MΩ. The extracellular solution contained (values are in mM): 150 NaCl, 2.8 KCl, 0.5 MgCl₂, 2 CaCl₂, 10 HEPES adjusted to pH 7.4 with NaOH. The pipette solution contains (values are in mM): 110 CsF, 30 CsCl, 4 NaCl, 0.5 CaCl₂, 10 Trypsin EDTA solution B (0.25%), EDTA (0.05%), 10 HEPES, adjusted to pH

7.2 with CsOH. Using double barrel glass (theta tube) glutamate and solutions of choice were rapidly administered, the theta tube was mounted on a high-speed piezo solution switcher (Automate Scientific, Berkeley, CA). After expelling the patch from the electrode to estimate the speed of solution exchange, the open tip potentials were recorded during the application of solutions of different ionic strengths. The 10%–90% solution exchange was typically at 500 ms. Data acquired were analyzed using Igor Pro7 (Wave Metrics, inc) (Li et al., 2003; Qneibi et al., 2019). AMPAR deactivation and desensitization were measured by applying glutamate (10 mM) for 1 ms and 500 ms, respectively. AMPAR-current deactivation and desensitization were fitted with two exponentials, and the weighted tau (τ_w) was calculated as $\tau_w = (\tau_f \times a_f) + (\tau_s \times a_s)$, where a_f and a_s are the relative amplitudes of the fast (τ_f) and slow (τ_s) exponential component.

4.9. Statistical Analysis

Significance compared with AMPAR expressed alone or with AMPAR+ Curcumin derivatives; p-value (one-way ANOVA): * < 0.05, ** < 0.01, *** < 0.001, ns – not significant

Acknowledgment

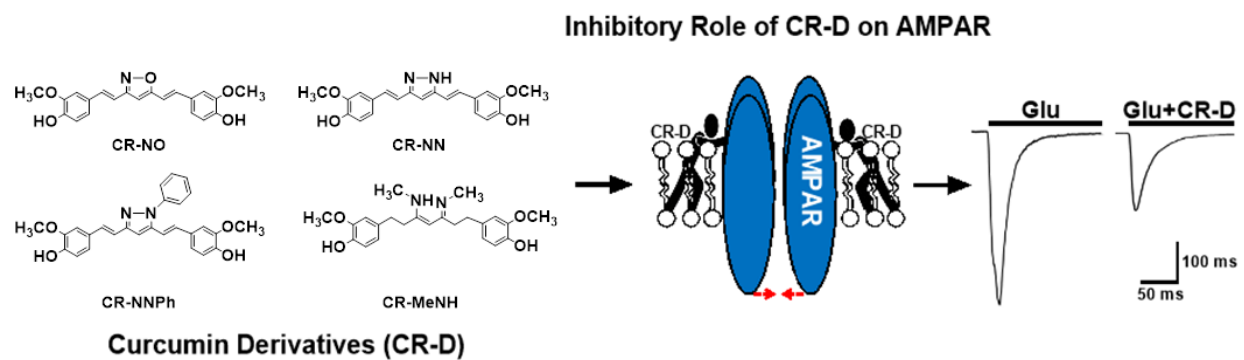
The work provided in this manuscript was supported by a grant from the Palestinian Ministry of Education and Higher Education (Grant number: ANNU-MoHE-1819-Sc017), thus the authors would like to acknowledge them in addition to An-Najah National University.

References

- Aggarwal, B., Kumar, A., S. Aggarwal, M., Shishodia, S., 2004. Curcumin Derived from Turmeric (*Curcuma longa*): a Spice for All Seasons. CRC Press Florida.
- Akhondzadeh, S., Abbasi, S.H., 2006. Herbal medicine in the treatment of Alzheimer's disease. *American journal of Alzheimer's disease and other dementias* 21, 113-118.
- Balannik, V., Menniti, F.S., Paternain, A.V., Lerma, J., Stern-Bach, Y., 2005. Molecular mechanism of AMPA receptor noncompetitive antagonism. *Neuron* 48, 279-288.
- Bertoncello, K.T., Aguiar, G.P.S., Oliveira, J.V., Siebel, A.M., 2018. Micronization potentiates curcumin's anti-seizure effect and brings an important advance in epilepsy treatment. *Sci. Rep.* 8, 2645-2645.
- Brody, H., Ames, D., Snowden, J., Woodward, M., Kirwan, J., Clarnette, R., Lee, E., Lyons, B., Grossman, F., 2003. A randomized placebo-controlled trial of risperidone for the treatment of aggression, agitation, and psychosis of dementia. *J. Clin. Psychiatry* 64, 134-143.
- Broughton, H.B., Watson, I.A., 2004. Selection of heterocycles for drug design. *J Mol Graph Model* 23, 51-58.
- Chang, P.K., Verbich, D., McKinney, R.A., 2012. AMPA receptors as drug targets in neurological disease--advantages, caveats, and future outlook. *The European journal of neuroscience* 35, 1908-1916.
- Chen, K., An, Y., Tie, L., Pan, Y., Li, X., 2015. Curcumin Protects Neurons from Glutamate-Induced Excitotoxicity by Membrane Anchored AKAP79-PKA Interaction Network. *Evid. Based Complement. Alternat. Med.* 2015, 706207.
- Collingridge, G.L., Olsen, R.W., Peters, J., Spedding, M., 2009. A nomenclature for ligand-gated ion channels. *Neuropharmacology* 56, 2-5.
- Esteban, J.A., 2003. AMPA receptor trafficking: a road map for synaptic plasticity. *Mol. Interv.* 3, 375-385.
- Hamed, O.A., Mehdawi, N., Taha, A.A., Hamed, E.M., Al-Nuri, M.A., Hussein, A.S., 2013. Synthesis and antibacterial activity of novel curcumin derivatives containing heterocyclic moiety. *Iran. J. Pharm. Res.* 12, 47-64.
- Hatcher, H., Planalp, R., Cho, J., Torti, F.M., Torti, S.V., 2008. Curcumin: from ancient medicine to current clinical trials. *Cell Mol. Life Sci.* 65, 1631-1652.
- Herguedas, B., Garcia-Nafria, J., Cais, O., Fernandez-Leiro, R., Krieger, J., Ho, H., Greger, I.H., 2016. Structure and organization of heteromeric AMPA-type glutamate receptors. *Science* 352, aad3873.
- Hollmann, M., Heinemann, S., 1994. Cloned glutamate receptors. *Annu. Rev. Neurosci.* 17, 31-108.
- Huang, Z., Li, G., Pei, W., Sosa, L.A., Niu, L., 2005. Enhancing protein expression in single HEK 293 cells. *J. Neurosci. Methods* 142, 159-166.
- Jayanarayanan, S., Smijin, S., Peeyush, K.T., Anju, T.R., Paulose, C.S., 2013. NMDA and AMPA receptor mediated excitotoxicity in cerebral cortex of streptozotocin induced diabetic rat: ameliorating effects of curcumin. *Chem. Biol. Interact.* 201, 39-48.
- Kew, J.N., Kemp, J.A., 2005. Ionotropic and metabotropic glutamate receptor structure and pharmacology. *Psychopharmacology (Berl)* 179, 4-29.
- Li, G., Pei, W., Niu, L., 2003. Channel-opening kinetics of GluR2Q(flip) AMPA receptor: a laser-pulse photolysis study. *Biochemistry* 42, 12358-12366.
- Libbey, J.E., Hanak, T.J., Doty, D.J., Wilcox, K.S., Fujinami, R.S., 2016. NBQX, a highly selective competitive antagonist of AMPA and KA ionotropic glutamate receptors, increases seizures and mortality following picornavirus infection. *Exp. Neurol.* 280, 89-96.
- Ma, H., Huang, Y., Cong, Z., Wang, Y., Jiang, W., Gao, S., Zhu, G., 2014. The efficacy and safety of atypical antipsychotics for the treatment of dementia: a meta-analysis of randomized placebo-controlled trials. *J. Alzheimers Dis.* 42, 915-937.

- Maheshwari, R.K., Singh, A.K., Gaddipati, J., Srimal, R.C., 2006. Multiple biological activities of curcumin: a short review. *Life Sci.* 78, 2081-2087.
- Matteucci, A., Cammarota, R., Paradisi, S., Varano, M., Balduzzi, M., Leo, L., Bellenchi, G.C., De Nuccio, C., Carnovale-Scalzo, G., Scordia, G., Frank, C., Mallozzi, C., Di Stasi, A.M., Visentin, S., Malchiodi-Albedi, F., 2011. Curcumin protects against NMDA-induced toxicity: a possible role for NR2A subunit. *Invest. Ophthalmol. Vis. Sci.* 52, 1070-1077.
- Menon, V.P., Sudheer, A.R., 2007. Antioxidant and anti-inflammatory properties of curcumin, The molecular targets and therapeutic uses of curcumin in health and disease. Springer, pp. 105-125.
- Nelson, K.M., Dahlin, J.L., Bisson, J., Graham, J., Pauli, G.F., Walters, M.A., 2017. The Essential Medicinal Chemistry of Curcumin. *J Med Chem* 60, 1620-1637.
- Nikam, S.S., Kornberg, B.E., 2001. AMPA receptor antagonists. *Curr. Med. Chem.* 8, 155-170.
- Qneibi, M., Jaradat, N., Hawash, M., Zaid, A.N., Natsheh, A.-R., Yousef, R., AbuHasan, Q., 2019. The Neuroprotective Role of *Origanum syriacum* L. and *Lavandula dentata* L. Essential Oils through Their Effects on AMPA Receptors. *J BioMed Research International.* 2019, 11.
- Qneibi, M.S., Micale, N., Grasso, S., Niu, L., 2012. Mechanism of inhibition of GluA2 AMPA receptor channel opening by 2,3-benzodiazepine derivatives: functional consequences of replacing a 7,8-methylenedioxy with a 7,8-ethylenedioxy moiety. *Biochemistry* 51, 1787-1795.
- Sanderson, D.J., Good, M.A., Seeburg, P.H., Sprengel, R., Rawlins, J.N., Bannerman, D.M., 2008. The role of the GluR-A (GluR1) AMPA receptor subunit in learning and memory. *Prog. Brain Res.* 169, 159-178.
- Schwenk, J., Harmel, N., Brechet, A., Zolles, G., Berkefeld, H., Muller, C.S., Bildl, W., Baehrens, D., Huber, B., Kulik, A., Klocker, N., Schulte, U., Fakler, B., 2012. High-resolution proteomics unravel architecture and molecular diversity of native AMPA receptor complexes. *Neuron* 74, 621-633.
- Seeburg, P.H., 1993. The TiPS/TINS lecture: the molecular biology of mammalian glutamate receptor channels. *Trends in pharmacological sciences* 14, 297-303.
- Shishodia, S., Sethi, G., Aggarwal, B.B., 2005. Curcumin: getting back to the roots. *Ann. N. Y. Acad. Sci.* 1056, 206-217.
- Simeone, T.A., Sanchez, R.M., Rho, J.M., 2004. Molecular biology and ontogeny of glutamate receptors in the mammalian central nervous system. *J. Child Neurol.* 19, 343-360; discussion 361.
- Singh, S.V., Hu, X., Srivastava, S.K., Singh, M., Xia, H., Orchard, J.L., Zaren, H.A., 1998. Mechanism of inhibition of benzo[a]pyrene-induced forestomach cancer in mice by dietary curcumin. *Carcinogenesis* 19, 1357-1360.
- Sobolevsky, A.I., Rosconi, M.P., Gouaux, E., 2009. X-ray structure, symmetry and mechanism of an AMPA-subtype glutamate receptor. *Nature* 462, 745-756.
- Sun, Y., Olson, R., Horning, M., Armstrong, N., Mayer, M., Gouaux, E., 2002. Mechanism of glutamate receptor desensitization. *Nature* 417, 245-253.
- Traynelis, S.F., Wollmuth, L.P., McBain, C.J., Menniti, F.S., Vance, K.M., Ogden, K.K., Hansen, K.B., Yuan, H., Myers, S.J., Dingledine, R., 2010. Glutamate receptor ion channels: structure, regulation, and function. *Pharmacol. Rev.* 62, 405-496.
- Twomey, E.C., Sobolevsky, A.I., 2018. Structural Mechanisms of Gating in Ionotropic Glutamate Receptors. *Biochemistry* 57, 267-276.
- Vickers, A., Zollman, C., Lee, R., 2001. Herbal medicine. *Western Journal of Medicine* 175, 125-128.
- Wang, C., Han, Y., Wu, A., Solyom, S., Niu, L., 2014. Mechanism and site of inhibition of AMPA receptors: pairing a thiazole with a 2,3-benzodiazepine scaffold. *ACS Chem. Neurosci.* 5, 138-147.
- Yelshanskaya, M.V., Singh, A.K., Sampson, J.M., Narangoda, C., Kurnikova, M., Sobolevsky, A.I., 2016. Structural Bases of Noncompetitive Inhibition of AMPA-Subtype Ionotropic Glutamate Receptors by Antiepileptic Drugs. *Neuron* 91, 1305-1315.

Graphical abstract



Highlights

- Over-activation of AMPA receptors is associated with various neurological diseases such as ALS, AD, epilepsy and strokes.
- The effect of newly synthesized curcumin derivatives on the homomeric GluA1 and heteromeric GluA1/A2 AMPA subunits were evaluated, encompassing effects on the whole cell current as well as the unique biophysical properties of AMPA.
- CR-MeNH and CR-NO increased desensitization and deactivation rates up to 3 folds, and resulted in highest level of inhibition.
- CR-NN, CR-NNPh decreased peak current by 4 folds, and prolonged both desensitization and deactivation states of both receptors.
- Curcumin, CR-PhCl, CR-PhF and CR-PhBr showed no significant impact on any of the tested biophysical properties nor possess any inhibitory actions.